Int. J. Heat Mass Transfer. Vol. 28, No. 11, pp. 2071–2077, 1985
Printed in Great Britain

0017-9310/85 $3.00 + 0.00
Pergamon Press Ltd.

Transition to the convective regime in a vertical slot

P. G. DANIELS

Department of Mathematics, The City University, Northampton Square, London EC1V 0HB, U.K.

(*Received* 22 *January* 1985 *and in final form* 20 *May* 1985)

Abstract—The break-down of the conductive regime in a laterally heated vertical slot is shown to be associated with the inward penetration of nonlinear convective effects from the ends of the slot. This penetration can occur in two quite distinct ways, depending on the Prandtl number of the fluid and the aspect ratio of the slot. At finite and small Prandtl numbers it takes the form of an imperfect bifurcation at a critical value of the Rayleigh number, leading to the establishment of a multiple-roll state throughout the slot. At larger Prandtl numbers there is a different transition process in which convective effects gradually penetrate inwards as the Rayleigh number increases. In this case the solution of an eigenvalue problem provides a quantitative measure of the transition, which leads to the so-called 'convective regime' in the slot.

1. INTRODUCTION

THE FLOW generated in a two-dimensional vertical slot by maintaining its sides at different constant temperatures has been widely studied following the theoretical work of Batchelor [1] and the experiments of Eckert and Carlson [2], Elder [3] and others. In recent years attention has focused on numerical simulations of the full Boussinesq equations governing the flow in the slot, [4–7], and relatively little work has been done to elucidate the formal asymptotic structure at large Rayleigh numbers. This is particularly true in relation to the complicated flow near the ends of the slot.

The general nature of the transition from the conductive regime described in [1] to the boundary-layer regime described by Gill [8] is well established and is described to some extent by an approximate solution introduced in [3] and later widely used as a basis for stability analyses of the flow [9–12]. However, this solution is a reasonable approximation only near the mid-level of the slot where horizontal velocities are small. Much less is known of the flow structure near the ends of the slot, although as the Rayleigh number is increased it is here that convective effects first become significant and subsequently penetrate into the core of the slot to produce a convective regime. From a mathematical viewpoint the value of the Prandtl number, σ, is found to have a crucial bearing on the character of the end-region solution and the nature of the penetration process. This is because at any *finite* value of σ the conductive solution is subject to a stationary instability which is forced by the end-zone dynamics, leading to an imperfect bifurcation and the propagation of multiple rolls into the core region of the slot. However, for *infinite* Prandtl number this instability is suppressed and a different type of penetration occurs in which the end zone subdivides into several distinct regions (Section 4). The outermost of these is governed by the vertical boundary-layer equations and it is this region that spreads and carries convective effects into the core of the slot. The vertical length scale associated with this process is found from the solution of an eigenvalue problem in Section 4 and this establishes a quantitative measure of the onset of the so-called 'convective regime'.

The flow is assumed to be two-dimensional. The quite different characteristics of the end-zone solution for finite and infinite Prandtl number are discussed in Section 3, and the structure of the solution in the latter case is analysed in Section 4. In practice, the assumption of infinite Prandtl number is less restrictive than might at first be imagined since even at moderate values of σ, conductive instabilities of both the stationary form (referred to above) and the travelling-wave type [10, 13] occur only at very high values of the Rayleigh number (see Section 3). Thus even at moderate values of σ the conductive base flow can give way to the more gradual penetration process associated with the infinite Prandtl number limit (Section 4) throughout the entire slot before the critical Rayleigh number for conductive instability is exceeded. This is discussed in greater detail in Section 5; in such circumstances the conductive instabilities are never relevant and the flow remains stable into the convective regime. This type of situation is consistent with the experimental observations of [3].

2. GOVERNING EQUATIONS

The slot is defined by the region $0 \leqslant x^* \leqslant l^*$, $0 \leqslant z^* \leqslant h^*$, with the vertical sidewalls $x^* = 0$ and $x^* = l^*$ maintained at constant temperatures T_0^* and $T_0^* + \Delta T^*$, respectively. Non-dimensional variables of temperature, velocity and length are defined by

$$T^* = T_0^* + \Delta T^* T(x, z) \tag{1}$$

$$(u^*, w^*) = \kappa(u, w)/l^* \tag{2}$$

$$(x^*, z^*) = l^*(x, z), \tag{3}$$

NOMENCLATURE

A	Rayleigh number	x, z	non-dimensional coordinates
A_c	critical Rayleigh number	x^*, z^*	coordinates
g	acceleration due to gravity	$\tilde{z}, \bar{z}$	scaled vertical coordinates.
h	aspect ratio of slot (height/width)		
h^*	slot height		
l^*	slot width	Greek symbols	
p	non-dimensional reduced pressure	$\alpha, \tilde{\alpha}$	eigenvalues of end-zone solution
T	non-dimensional temperature	β	coefficient of thermal expansion
T_c	non-dimensional core temperature	θ, ϕ	eigenfunctions of end-zone solution
$\tilde{T}, \bar{T}$	scaled temperatures	κ	thermal diffusivity
T^*	temperature	ν	kinematic viscosity
T_0^*	temperature of cold wall	σ	Prandtl number
ΔT^*	temperature difference across slot	ψ	non-dimensional stream function
u, w	non-dimensional velocity components	ψ_c	non-dimensional core stream function
u^*, w^*	velocity components	$\tilde{\psi}, \bar{\psi}$	scaled stream functions.

where κ is the thermal diffusivity. The Boussinesq equations governing the steady motion of the fluid are then given by

$$\frac{\partial u}{\partial x}+\frac{\partial w}{\partial z}=0 \tag{4}$$

$$\sigma^{-1}\left(u\frac{\partial u}{\partial x}+w\frac{\partial u}{\partial z}\right)=-\frac{\partial p}{\partial x}+\nabla^2 u \tag{5}$$

$$\sigma^{-1}\left(u\frac{\partial w}{\partial x}+w\frac{\partial w}{\partial z}\right)=-\frac{\partial p}{\partial z}+\nabla^2 w+AT \tag{6}$$

$$u\frac{\partial T}{\partial x}+w\frac{\partial T}{\partial z}=\nabla^2 T, \tag{7}$$

where p is the non-dimensional reduced pressure. The Prandtl number σ and the Rayleigh number A are defined by

$$\sigma=\nu/\kappa, \quad A=\beta g\Delta T^* l^{*3}/\kappa\nu, \tag{8}$$

where ν is the kinematic viscosity and β is the coefficient of thermal expansion.

The boundary conditions on the vertical sidewalls are

$$\left.\begin{aligned} u=w=T=0 \quad & \text{on } x=0 \\ u=w=0, \quad T=1 \quad & \text{on } x=1 \end{aligned}\right\} \tag{9}$$

and the horizontal walls are assumed to be adiabatic so that

$$u=w=\frac{\partial T}{\partial z}=0 \quad \text{on } z=0 \text{ and } z=h, \tag{10}$$

where $h=h^*/l^*$ is the vertical aspect ratio of the slot. A stream function ψ is also introduced where

$$u=\frac{\partial \psi}{\partial z}, \quad w=-\frac{\partial \psi}{\partial x}. \tag{11}$$

The motion in the slot is controlled by the three parameters σ, A and h. The present work is concerned chiefly with the structure of the flow near the ends of the slot when h is large.

3. THE END-ZONE STRUCTURE

The flow in the slot is characterised by several different regimes which are identified by the relative sizes of the Rayleigh number, A, and the aspect ratio, h, the latter being assumed large. The first of these corresponds to A of $O(1)$ when the core flow throughout most of the slot is the conductive solution

$$T=T_c, \quad \psi=A\psi_c, \tag{12}$$

where

$$T_c=x, \quad \psi_c=\frac{x^2}{24}(1-x)^2. \tag{13}$$

This linear solution, originally given in [1], is actually an exact solution of the full equations (4)–(7), representing an anti-symmetric vertical motion with fluid ascending in the hotter half of the slot ($x>\frac{1}{2}$) and descending in the cooler half ($x<\frac{1}{2}$). Near the ends of the slot the fluid must be turned and the solution (12) is clearly invalid. Since the overall motion can be assumed centro-symmetric (see [8]) only the solution at the lower end of the slot need be considered, and it is clear that if A is of $O(1)$, the motion in the end zone $0\leqslant x\leqslant 1$, $0\leqslant z\leqslant\infty$ is governed by the full nonlinear Boussinesq equations (4)–(7) with boundary conditions given by (9) on $x=0$ and $x=1$ and by

$$\psi=\frac{\partial \psi}{\partial z}=\frac{\partial T}{\partial z}=0 \quad \text{on } z=0. \tag{14}$$

The motion is generated by the final condition

$$\psi\to A\psi_c, \quad T\to T_c \quad \text{as } z\to\infty, \tag{15}$$

which must be satisfied if the solution is to match with the core solution (12).

Thus the regime where A is of $O(1)$ is identified by the presence of nonlinear inertial and convective effects in roughly square zones at each end of the slot and the flow is determined by solutions of the full Boussinesq equations subject to (9), (14) and (15). Although it is hoped that a numerical scheme similar to that used by Hart [14] in a related problem will eventually provide detailed flow patterns for different values of σ and A, the aim of the present paper is to identify the main features of the solution and in particular the development of the end-zone structure as $A \to \infty$, when, in the limit of infinite Prandtl number, convective effects first begin to influence the core flow (Section 4).

The opposite limit, $A \to 0$, is of less interest since then the flow throughout the entire slot is linear. The end-zone solution can be expanded as

$$T = T_c + AT_1 + \ldots, \quad \psi = A(\psi_c + \psi_1) + \ldots, \tag{16}$$

where, from (4)–(6), ψ_1 satisfies the biharmonic equation

$$\nabla^4 \psi_1 = 0, \tag{17}$$

with boundary conditions

$$\begin{aligned} &\psi_1 = \frac{\partial \psi_1}{\partial x} = 0 && \text{on } x = 0 \text{ and } x = 1 \\ &\psi_1 = -\psi_c, \quad \frac{\partial \psi_1}{\partial z} = 0 && \text{on } z = 0 \\ &\psi_1 \to 0 && \text{as } z \to \infty. \end{aligned} \tag{18}$$

The solution can be expressed as a sum of exponentials $\exp(-\alpha z)$ whose coefficients are eigenfunctions in x associated with (complex) eigenvalues α. The properties of this type of solution of the biharmonic equation have already been discussed in detail [15–18]. The solution for ψ_1 is clearly an even function of $x - \frac{1}{2}$.

Once ψ_1 is determined, the heat equation (7) is used to obtain the first correction to the temperature field, T_1, which is the solution of

$$\nabla^2 T_1 = \frac{\partial \psi_1}{\partial z}, \tag{19}$$

subject to

$$\begin{aligned} &T_1 = 0 \text{ on } x = 0 \text{ and } x = 1, \\ &\frac{\partial T_1}{\partial z} = 0 \text{ on } z = 0, \quad T_1 \to 0 \text{ as } z \to \infty. \end{aligned} \tag{20}$$

The expansions (16) can be further extended in a straightforward manner.

One fundamental property of the end-zone problem at *general* values of A concerns the nature of the decay of the solution to the outer boundary conditions (15). As $z \to \infty$, solutions that satisfy (15) have asymptotic forms

$$\begin{aligned} &T \sim T_c + \theta(x) \exp(-\alpha z), \\ &\psi \sim A\{\psi_c + \phi(x) \exp(-\alpha z)\}, \end{aligned} \tag{21}$$

where the possible values of α are the solutions of the eigenvalue problem

$$\theta'' + \alpha^2 \theta = \alpha A(\psi_c' \theta - \phi) \tag{22}$$

$$\phi'''' + 2\alpha^2 \phi'' + \alpha^4 \phi = \theta' + \frac{\alpha A}{\sigma} \{(\alpha^2 \psi_c' - \psi_c''')\phi + \psi_c' \phi''\} \tag{23}$$

$$\theta = \phi = \phi' = 0 \quad \text{on } x = 0 \text{ and } x = 1, \tag{24}$$

obtained from linearisation of (4)–(7). It is easily shown that if α, $\theta(x)$, $\phi(x)$ are solutions of (22)–(24) then so are $-\alpha$, $\theta(1-x)$, $-\phi(1-x)$ and, for complex α, so also are α^*, $\theta^*(x)$, $\phi^*(x)$ where * denotes complex conjugate.

The asymptotic forms (21) are consistent with a complete solution of the end-zone problem only if the system (22)–(24) has a triply-infinite set of eigenvalues with positive real part. This is certainly true for small values of A where, as $A \to 0$, there is one set of real eigenvalues obtained essentially from the LHS of (22) and given by

$$\alpha \sim n\pi, \quad \theta \sim \sin n\pi x, \quad \phi = O(1), \quad (n = 1, 2 \ldots) \tag{25}$$

and two further sets which are the complex conjugate solutions with positive real part of

$$\sin^2 \alpha - \alpha^2 = 0. \tag{26}$$

The latter solutions correspond to the eigenfunctions

$$\phi \sim \sin \alpha x - \alpha x \cos \alpha x + (\alpha \cot \alpha - 1) x \sin \alpha x, \tag{27}$$

associated with the LHS of (23); even solutions for ϕ correspond to the complex roots of $\sin \alpha + \alpha = 0$, which have been tabulated by Robbins and Smith [19], while the odd solutions correspond to the complex roots of $\sin \alpha - \alpha = 0$ tabulated by Hillman and Salzer [20]. The leading eigenvalues are associated with an even eigensolution and are given by

$$\alpha = 4.21 \pm 2.26\mathrm{i}. \tag{28}$$

Further properties of these eigenfunctions have been derived in connection with the solution of the biharmonic equation in a semi-infinite strip, [15–18], with applications in elastic structures as well as fluid flow [21]. In the present problem the results are relevant only as $A \to 0$ and it is only in this limit that the eigenfunctions of (22)–(24) divide naturally into even and odd sets.

For higher values of A solutions must be obtained by numerical means but some crucial information can be inferred from stability analyses of the conductive solution (12) in an infinite vertical layer. The eigenvalue problem (22)–(24) is precisely that obtained in the analysis of the stability of the system to (transverse) stationary disturbances [9, 22, 23] although there, of course, interest centres on solutions with α purely imaginary. The first purely imaginary root (as A increases) occurs at

$$A = A_c \approx 7880\sigma, \tag{29}$$

and this result appears to be valid (to within a few

percent) for all Prandtl numbers (see [9, 12]); for $A > A_c$ the system (22)–(24) has purely imaginary solutions for α that generate the neutral curve given in [9]. In the present context this implies that the necessary triply-infinite set of eigenvalues with positive real part does not exist for $A > A_c$ and a solution of the end-zone equations satisfying (15) is no longer possible. As A increases beyond A_c the short length-scale rolls associated with the instability are forced into the core zone, destroying the conductive state given by (12). This is an example of a smooth transition (or imperfect bifurcation) to a multiple-roll state throughout the slot; similar situations have been analysed in Rayleigh–Bénard convection [24–26] and Taylor–Couette flow [27].

Although the present work is concerned only with the basic steady-state solution in the slot, it should be added that the results of [10] indicate that a (perfect) bifurcation to a travelling-wave state would be expected when

$$A \sim 9400\sigma^{1/2} \quad (\sigma \gg 1), \tag{30}$$

which is actually a lower critical Rayleigh number than that for the onset of the stationary instability (29) when the Prandtl number is large. Further results for finite Prandtl numbers, [13], have actually established that the travelling-wave disturbances have a lower critical Rayleigh number if $\sigma > 12.7$.

In view of the above considerations, it is interesting to note that in Elder's experiments [3] the end zones were explicitly observed to be regions of strong damping and secondary-roll motions were always seen first near the centre of the slot. However, the experiments were performed with fluids of large Prandtl number ($\sigma \approx 10^3$) indicating the possibility that neither of the conditions (29) or (30) is met before the conductive solution is destroyed by the more gradual penetration of convective effects into the core region associated with the limiting process $A \to \infty$. Mathematically, this situation can be modelled by the assumption that $\sigma = \infty$ so that neither of the conditions (29) or (30) is ever met; the end zones remain passive for all values of A and a possible structure for the solution as $A \to \infty$ can be proposed (Section 4) and used to estimate the penetration of convective effects into the core. The vertical scale of the core, h, becomes an important limiting factor in this process and in practical situations (Section 5) it is the size of σ relative to h that determines whether the onset of the convective regime occurs in this way, rather than through the imperfect bifurcation process described above.

A numerical solution of the eigenvalue problem (22)–(24) for the case $\sigma = \infty$ using a Runge–Kutta scheme confirmed the absence of purely imaginary roots (α, which would correspond to the stationary instability of the basic state) for all values of A. The first two of the triply-infinite set of eigenvalues with positive real part are shown in Fig. 1. Each set has one real branch and a pair of complex conjugate branches. The complex roots, which stem from the solutions of (26) at $A = 0$, remain finite as $A \to \infty$, while the real roots, which stem from the values (25), decay to zero. This latter behaviour is associated with the convective penetration process and is discussed in detail in the next section.

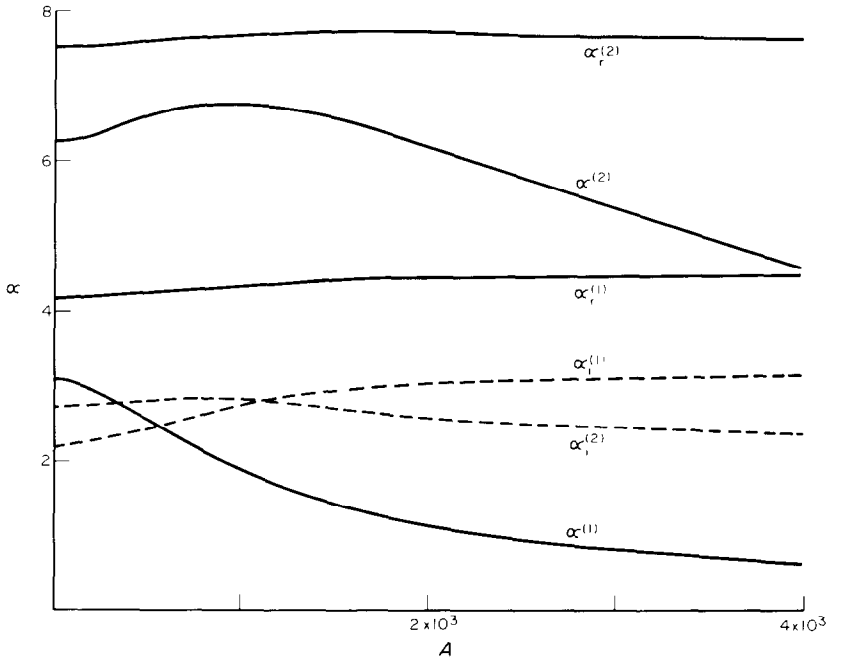

FIG. 1. The first two sets of eigenvalues α as a function of Rayleigh number, A, for infinite Prandtl number. Real roots are $\alpha^{(1)}$, $\alpha^{(2)}$. Complex roots are $\alpha_r^{(1)} + i\alpha_i^{(1)}$, $\alpha_r^{(2)} + i\alpha_i^{(2)}$.

4. THE END-ZONE STRUCTURE AS $A \to \infty$ AT INFINITE PRANDTL NUMBER

In the limit of infinite Prandtl number the end-zone equations (4)–(7) reduce to the form

$$\nabla^4\psi = A\frac{\partial T}{\partial x}, \quad \nabla^2 T = \frac{\partial(T,\psi)}{\partial(x,z)}, \tag{31}$$

and a structure is required for $A \gg 1$ consistent with the outer conditions

$$T \to T_c, \quad \psi \to A\psi_c \quad \text{as } z \to \infty. \tag{32}$$

These forms for T and ψ and the need to maintain a balance in the heat equation, indicate a main outer zone where $\tilde{z} = A^{-1}z$ is of $O(1)$ and

$$T \sim \tilde{T}(x,\tilde{z}), \quad \psi \sim A\tilde{\psi}(x,\tilde{z}), \tag{33}$$

where the governing equations are the vertical boundary-layer equations

$$\frac{\partial^4\tilde{\psi}}{\partial x^4} = \frac{\partial\tilde{T}}{\partial x}, \quad \frac{\partial^2\tilde{T}}{\partial x^2} = \frac{\partial(\tilde{T},\tilde{\psi})}{\partial(x,\tilde{z})}. \tag{34}$$

These must be solved subject to

$$\left.\begin{aligned} \tilde{\psi} = \frac{\partial\tilde{\psi}}{\partial x} = \tilde{T} = 0 \quad & \text{on } x = 0 \\ \tilde{\psi} = \frac{\partial\tilde{\psi}}{\partial x} = 0, \quad \tilde{T} = 1 \quad & \text{on } x = 1 \end{aligned}\right\} \tag{35}$$

$$\tilde{\psi} \to \psi_c, \quad \tilde{T} \to T_c \quad \text{as } \tilde{z} \to \infty, \tag{36}$$

and, tentatively,

$$\tilde{\psi} = 0 \quad \text{on } \tilde{z} = 0. \tag{37}$$

It is expected that this last condition is needed to ensure a consistent solution near the horizontal wall, $z = 0$. The full conditions (14) cannot be satisfied because the highest derivatives in z are neglected in the equations (34) and the necessary adjustments must be provided by thinner horizontal layers. Asymptotic solutions of the vertical boundary-layer equations by Blythe *et al.* [28] suggest that the solutions of (34) subject to (35) and (37) have the behaviour

$$\tilde{\psi} \sim a\tilde{z}^{3/5}, \quad \tilde{T} \sim b\tilde{z}^{3/10} \quad \text{as } \tilde{z} \to 0, \tag{38}$$

for $0 < x < 1$.

The horizontal momentum balance in (31) then suggests that an outer horizontal layer exists where z is of $O(A^{-3/37})$. Appropriate local variables for this layer are $\bar{z}$, $\bar{\psi}$ and $\bar{T}$ where

$$z = A^{-3/37}\bar{z}, \quad \psi \sim A^{13/37}\bar{\psi}, \quad T \sim A^{-12/37}\bar{T}. \tag{39}$$

Then, from (31),

$$\frac{\partial^4\bar{\psi}}{\partial\bar{z}^4} = \frac{\partial\bar{T}}{\partial x}, \tag{40}$$

and, since the convective terms dominate in the heat equation,

$$\bar{T} = \bar{T}(\bar{\psi}). \tag{41}$$

This suggests the need for a further inner thermal layer in order to achieve the temperature condition at the base wall. Provided that the solution of (40) and (41) satisfies $\bar{\psi} = O(\bar{z}^2)$ as $\bar{z} \to 0$, the heat equation infers that this layer has thickness z of $O(A^{-19/111})$.

The complete solution of the horizontal layers requires a careful analysis of the flow in each corner of the end zone and this is deferred for future consideration. The main aim of the present work is to determine a quantitative measure of the size of the outer zone where z is of $O(A)$ since this will, in turn, provide an accurate estimate of the range of validity of the conductive solution in the slot.

The vertical decay scale associated with the outer zone is found by setting

$$\tilde{T} = T_c + \theta(x)\exp(-\tilde{\alpha}\tilde{z}), \quad \tilde{\psi} = \psi_c + \phi(x)\exp(-\tilde{\alpha}\tilde{z}). \tag{42}$$

Substitution into (34) and linearisation gives the reduced eigenvalue problem

$$\phi'''' = \theta' \tag{43}$$

$$\theta'' - \tilde{\alpha}(\psi_c'\theta - \phi) = 0 \tag{44}$$

$$\theta = \phi = \phi' = 0 \quad \text{on } x = 0 \text{ and } x = 1. \tag{45}$$

The same system can be derived from the full eigenvalue problem (22)–(24) by setting $\sigma = \infty$ and letting $A \to \infty$ with $\alpha \sim \tilde{\alpha}/A$. A numerical solution of (43)–(45) gave the first three eigenvalues as

$$\tilde{\alpha} = 2.58 \times 10^3, \quad 2.31 \times 10^4, \quad 5.76 \times 10^4. \tag{46}$$

The first two solutions correspond to the asymptotic behaviour (as $A \to \infty$) of the two real branches shown in Fig. 1. The eigenfunctions θ and ϕ associated with the leading eigenvalue are shown in Fig. 2. The reason for the large values of $\tilde{\alpha}$ in (46) can be seen from a simple WKB approximation to the system (43)–(45). Although the full problem is rather complicated the dominant balance [which is between the first two terms on the LHS of (44)] suggests a family of eigensolutions in which

$$\tilde{\alpha}^{1/2}\int_{1/2}^{1}(-\psi_c')^{1/2}\,dx \sim n\pi \quad \text{as } n \to \infty, \tag{47}$$

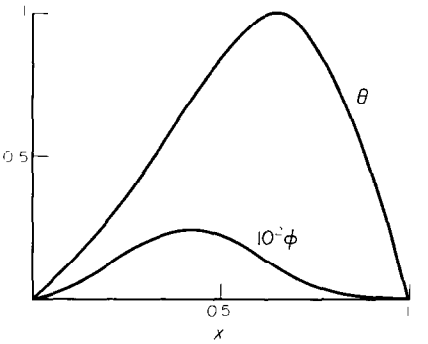

FIG. 2. The eigenfunctions θ and ϕ associated with the leading eigenvalue $\tilde{\alpha} = 2.58 \times 10^3$.

where n is an integer. The small numerical value of the integral,

$$\int_{1/2}^{1} (-\psi_c')^{1/2}\, dx = 0.0346, \tag{48}$$

then leads to the result that for large n successive values of $\tilde{\alpha}^{1/2}$ should be separated by approx. 90.8. This compares very favourably with the actual values

$$\tilde{\alpha}^{1/2} = 50.8, 152, 240 \tag{49}$$

obtained from (46).

The leading eigenvalue in (46) determines the length scale associated with the outer convective zone; a double e-folding scale representing a decay to within about 13.5% of the limiting form is

$$z \sim 2A/\tilde{\alpha} = A/1290, \tag{50}$$

and, based on this, the convective end zones effectively replace the conductive solution throughout the slot when

$$h/2 \sim A/1290. \tag{51}$$

Thus the conductive regime is completely destroyed when

$$A \gtrsim 645h. \tag{52}$$

5. DISCUSSION

The end-zone penetration measured by the condition (52) leads to the second significant flow regime in the slot; this is the convective regime where the Rayleigh number and aspect ratio are such that

$$A = O(h). \tag{53}$$

The analysis of Section 4 suggests that in the infinite Prandtl number limit the basic state is governed by the vertical boundary-layer equations (34), but now to be solved in the finite region $0 \leqslant x \leqslant 1$, $0 \leqslant \tilde{z} \leqslant h/A$ subject to (35) and the end conditions

$$\tilde{\psi} = 0 \text{ on } \tilde{z} = 0 \text{ and } \tilde{z} = h/A. \tag{54}$$

As $A/h \to 0$, the conductive solution is recovered as the end zones revert back to the short z length scale at each end of the slot, while (stability considerations apart) the limit $A/h \to \infty$ should see the development of the boundary-layer regime envisaged in [8], with distinct vertical layers on each sidewall and a vertically stratified horizontal shear flow across the core. The significance of the parameter regime in which A is of $O(h)$ has already been recognised in the analysis of [3] and subsequent work, although numerical solutions ([4–7], for example) have been based on the full Boussinesq equations (4)–(7) rather than the reduced problem of solving (34) subject to (35) and (54). In the infinite Prandtl number limit it is this regime where destabilisation occurs and the interesting features associated with secondary and tertiary flows [3] are observed. The condition (54) would seem to be consistent with the comment in [3] that these motions are not connected with end effects.

Finally, comparison of (52), (29) and (30) shows that at large Prandtl numbers the conductive instabilities are only likely to be relevant in slots for which

$$h > 12.2\sigma \quad \text{(stationary modes)}, \tag{55}$$

or

$$h > 14.6\sigma^{1/2} \quad \text{(oscillatory modes)}. \tag{56}$$

It should be noted that these results are based on the failure of the conductive solution throughout the entire slot. According to the analysis of Section 4, the conductive solution remains intact longest in the vicinity of the mid-level of the slot as the Rayleigh number is increased, and conditions for the validity of the conductive solution near the *ends* of the slot would require even larger numerical factors in (55) and (56). The results (55), (56) are consistent with the absence of the conductive instability in the experiments of [3] where the Prandtl number was typically of the order of 10^3. The oscillatory mode would require a slot with vertical aspect ratio $h \gtrsim 462$ while the stationary mode would require $h \gtrsim 12{,}200$. If (52) is also assumed applicable at lower Prandtl numbers (where the stationary instability is preferred) the result (55) will still be relevant since the condition for stationary instability is given by (29) for virtually all Prandtl numbers. The conductive instability is then predicted to occur in a water-filled slot ($\sigma = 7.1$) if $h \gtrsim 87$ and in an air-filled slot ($\sigma = 0.72$) if $h \gtrsim 8.8$.

REFERENCES

1. G. K. Batchelor, Heat transfer by free convection across a closed cavity between vertical boundaries at different temperatures, *Q. Jl appl. Math.* **12**, 209–233 (1954).
2. E. R. G. Eckert and W. O. Carlson, Natural convection in an air layer enclosed between two vertical plates with different temperatures, *Int. J. Heat Mass Transfer* **2**, 106–120 (1961).
3. J. W. Elder, Laminar free convection in a vertical slot, *J. Fluid Mech.* **23**, 77–98 (1965).
4. J. W. Elder, Numerical experiments with free convection in a vertical slot, *J. Fluid Mech.* **24**, 823–843 (1966).
5. I. Catton, P. S. Ayyaswamy and R. M. Clever, Natural convection in a finite, rectangular slot arbitrarily oriented with respect to the gravity vector, *Int. J. Heat Mass Transfer* **17**, 173–184 (1974).
6. N. Seki, S. Fukusako and H. Inaba, Visual observations of natural convective flow in a narrow vertical cavity, *J. Fluid Mech.* **84**, 695–704 (1978).
7. P. Bontoux and B. Roux, Numerical approaches in natural convection, Von Karman Institute for Fluid Dynamics: Lecture series 9. Natural convection: theory and experiment (1982).
8. A. E. Gill, The boundary layer regime for convection in a rectangular cavity, *J. Fluid Mech.* **26**, 515–536 (1966).
9. C. M. Vest and V. S. Arpaci, Stability of natural convection in a vertical slot, *J. Fluid Mech.* **36**, 1–15 (1969).
10. A. E. Gill and C. C. Kirkham, A note on the stability of convection in a vertical slot, *J. Fluid Mech.* **42**, 125–127 (1970).
11. J. E. Hart, Stability of flow in a differentially heated inclined box, *J. Fluid Mech.* **47**, 547–576 (1971).

12. R. F. Bergholz, Instability of steady natural convection in a vertical fluid layer, *J. Fluid Mech.* **84,** 743–768 (1978).
13. S. A. Korpela, D. Gozum and C. B. Baxi, On the stability of the conductive regime of natural convection in a vertical slot, *Int. J. Heat Mass Transfer* **16,** 1683–1690 (1973).
14. J. E. Hart, Low Prandtl number convection between differentially heated end walls, *Int. J. Heat Mass Transfer* **26,** 1069–1074 (1983).
15. R. C. T. Smith, The bending of a semi-infinite strip, *Aust. J. scient. Res.* **5,** 227–237 (1952).
16. M. W. Johnson and R. W. Little, The semi-infinite elastic strip, *Q. Jl Appl. Math.* **22,** 335–344 (1964).
17. D. D. Joseph, The convergence of biorthogonal series for biharmonic and Stokes flow edge problems, Part I, *SIAM J. appl. Math.* **33,** 337–347 (1977).
18. D. D. Joseph and L. Sturges, The convergence of biorthogonal series for biharmonic and Stokes flow edge problems, Part II, *SIAM J. appl. Math.* **34,** 7–26 (1978).
19. C. I. Robbins and R. C. T. Smith, A table of roots of $\sin z = -z$, *Phil. Mag.* **39,** 1005 (1948).
20. A. P. Hillman and H. E. Salzer, Roots of $\sin z = z$, *Phil. Mag.* **34,** 575 (1943).
21. H. K. Moffatt, Viscous and resistive eddies near a sharp corner, *J. Fluid Mech.* **18,** 1–18 (1964).
22. G. E. Gershuni, On the stability of plane convective motion of a liquid, *Zh. tekh. Fiz.* **23,** 1838–1844 (1953).
23. R. N. Rudakov, Spectrum of perturbations and stability of convective motion between vertical planes, *Prikl. Mat. Mekh.* **31,** 349–355 (1967).
24. P. G. Daniels, The effect of distant sidewalls on the transition to finite amplitude Bénard convection, *Proc. R. Soc.* **A358,** 173–197 (1977).
25. P. Hall and I. C. Walton, The smooth transition to the convective regime in a two-dimensional box, *Proc. R. Soc.* **A358,** 199–221 (1977).
26. K. Stewartson and M. Weinstein, Marginal convection in a large rigid box, *Phys. Fluids* **22,** 1421–1427 (1979).
27. R. Graham and J. A. Domaradzki, Local amplitude equation of Taylor vortices and its boundary condition, *Phys. Rev.* **A26,** 1572–1579 (1982).
28. P. A. Blythe, P. G. Daniels and P. G. Simpkins, Thermal convection in a cavity: the core structure near the horizontal boundaries, *Proc. R. Soc.* **A387,** 367–388 (1983).

TRANSITION AU REGIME DE CONVECTION DANS UNE FENTE VERTICALE

Résumé—La cessation du régime conductif dans une fente verticale chauffée latéralement est associée à la pénétration des effets convectifs non linéaires à partir des extrémités. Cette pénétration peut se faire de deux façons entièrement différentes, selon le nombre de Prandtl du fluide et le rapport de forme de la fente. Aux petits nombres finis de Prandtl elle prend la forme d'une bifurcation imparfaite à la valeur critique du nombre de Rayleigh, conduisant à l'établissement d'un état multicellulaire à travers la fente. Aux plus grands nombres de Prandtl, il y a un mécanisme de transition dans lequel les effets convectifs pénètrent graduellement lorsque le nombre de Rayleigh augmente. Dans ce cas, la solution d'un problème à valeurs propres fournit une mesure quantitative de la transition que conduit au 'régime de convection' dans la fente.

DAS EINSETZEN VON KONVEKTION IN EINEM SENKRECHTEN SPALT

Zusammenfassung—Es wird gezeigt, daß das Zusammenbrechen der reinen Wärmeleitung in einem seitlich beheizten senkrechten Spalt mit dem Eindrigen von nichtlinearen Konvektionseffekten vom Ende des Spalts her zusammenhängt. Dieses Eindringen kann auf zwei sehr unterschiedliche Arten auftreten, je nach Prandtl-Zahl des Fluids und Längen- zu Dicken-Verhältnis des Spalts. Bei endlich kleinen Prandtl-Zahlen nimmt es die Form einer unvollständigen Gabelung an, wenn ein kritischer Wert der Rayleigh-Zahl erreicht ist. Dies führt zum Entstehen von mehrfachen Konvektionswalzen im gesamten Spalt. Bei größeren Prandtl-Zahlen findet der Übergang durch allmähliches Vordringen der Konvektionseffekte mit zunehmender Rayleigh-Zahl statt. In diesem Fall führt die Lösung des Eigenwertproblems zu einem quantitativen Maß für den Übergang, was zum sogenannten 'Konvektionsgebiet' im Spalt führt.

ПЕРЕХОД К КОНВЕКТИВНОМУ РЕЖИМУ В ВЕРТИКАЛЬНОЙ ЩЕЛИ

Аннотация—Показано, что нарушение режима теплопроводности в нагреваемой сбоку вертикальной щели связано с развитием внутри щели нелинейной конвекции, обусловленной концевыми эффектами. Это развитие может происходить двумя различными способами, зависящими от числа Прандтля жидкости и отношения сторон щели. При конечном и малом числах Прандтля оно приводит к бифуркации, когда при критическом значении числа Рэлея устанавливается режим с ячеистой структурой по всей щели. При больших числах Прандтля существует другой переходный процесс, при котором с ростом числа Рэлея влияние конвективных эффектов увеличивается. В этом случае решение задачи на отыскание собственных значений обеспечивает качественный критерий переходного режима, который приводит к так называемому 'конвективному режиму' в щели.